Supplementary material

For

Degradation of ciprofloxacin in UV/NH_2Cl process: kinetics, mechanism, pathways and DBPs formation

Ruihua Zhang[a1], Cheng Peng[a1], Qiongfang Wang[a*], Xinyu Zou[a], Qiming Zhao[a], Jiajun Wang[a], Jiayu Zhang[a], Lei Dong[b, c], Xin Zhang[c], Naiyun Gao[b]

[a] College of Chemistry and Chemical Engineering, Shanghai University of Engineering Science, Shanghai 201600, China

[b] State Key Laboratory of Pollution Control Reuse, Tongji University, Shanghai 200092, China

[c] Shanghai Municipal Engineering Design Institute (Group) Co., LTD, Shanghai 200092, China

[1] Co-first authors

Tables

Table S1. Trihalomethanes and haloacetonitriles analysis – gas chromatograph operating conditions

Parameter	**Description**
Injector Temperature	Splitless 200°C
	15 sec purge activation time
Detector Temperature	300°C
Temperature Program	35°C for 9.0 min
	10°C/min temperature ramp to 40°C
	40°C for 3.0 min
	15°C/min temperature ramp to 150°C
	150°C for 1.0 min
Carrier Gas	Helium
Flow Rate	24.8 cm/sec at 150°C

Table S2. Haloacetic acids analysis – gas chromatograph operating conditions

Parameter	**Description**
Injector Temperature	Splitless 210°C
	15 sec purge activation time
Detector Temperature	300°C
Temperature Program	40°C for 2.0 min
	1°C/min temperature ramp to 65°C
	65°C for 2.0 min
	10°C/min temperature ramp to 90°C
	150°C for 0 min
	30°C/min temperature ramp to 210°C
	210°C for 2.0 min
Carrier Gas	Helium
Flow Rate	24.8 cm/sec at 150°C

Table S3. Comparison of degradation efficiency between different systems

Degradation system	**Target pollution**	**Initial concentration**	**UV lamp power**	**Oxidant concentration**	**Degradation time**	**Reference**
UV/Cl_2	Metoprolol	0.1 mg/L	1.1 mW/cm^2	1.0 mM	120 min	(Nam et al. 2015)
UV/H_2O_2	Cefixime	9 mg/L	36 W	0.85 mM	180 min	(Belghadr et al. 2014)
UV/PS	Thiamphenicol	0.14 mg/L	20 W	1.0 mM	60 min	(Wang et al. 2017)
UV/NH_2Cl	Ciprofloxacin	5 mg/L	65 uW/cm^2	0.5 mM	90 min	/

Reference

[1] Belghadr, Issa, Ghodratollah Shams Khorramabadi, Hatam Godini, and Mohammad Almasian. 2014. 'The removal of the cefixime antibiotic from aqueous solution using an advanced oxidation process (UV/H2O2)', *Desalination and Water Treatment*, 55: 1068-75.

[2] Nam, S. W., Y. Yoon, D. J. Choi, and K. D. Zoh. 2015. 'Degradation characteristics of metoprolol during UV/chlorination reaction and a factorial design optimization', *J Hazard Mater*, 285: 453-63.

[3] Wang, Feige, Wenjing Wang, Shoujun Yuan, Wei Wang, and Zhen-Hu Hu. 2017. 'Comparison of UV/H2O2 and UV/PS processes for the degradation of thiamphenicol in aqueous solution', *Journal of Photochemistry and Photobiology A: Chemistry*, 348: 79-88.

Table S4. pH change of UV/NH_2Cl system in pH experiments

	pH				
Before reaction	3.0	5.0	7.0	9.0	11.0
After reaction (Parallel experiment I)	3.12	5.89	6.26	6.85	8.76
After reaction (Parallel experiment II)	3.25	5.74	6.13	7.23	9.12

Table S5. Degradation products of CIP during the UV/NH_2Cl process

Compound	Retention Time(min)	m/z	Formula	Possible chemical structure
CIP	3.59	311.13	$C_{17}H_{18}FN_3O_3$	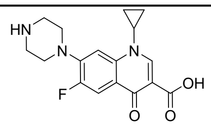
A	3.18	305.12	$C_{15}H_{16}FN_3O_3$	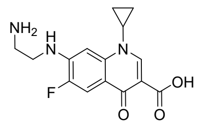
B	6.98	262.08	$C_{13}H_{11}FN_2O_3$	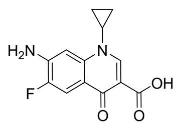
C	1.61	248.10	$C_{13}H_{13}FN_2O_2$	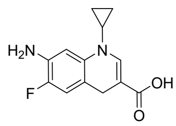
D	1.61	204.11	$C_{12}H_{13}FN_2$	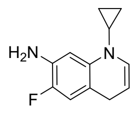

E	3.48	146.08	$C_9H_{12}N_2$	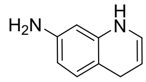
F	5.57	361.11	$C_{17}H_{16}FN_3O_5$	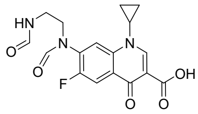
G	3.79	244.06	$C_{13}H_9FN_2O_2$	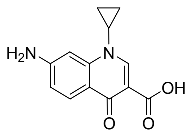
H	5.45	291.10	$C_{14}H_{14}FN_3O_3$	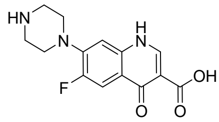
I	6.98	265.09	$C_{12}H_{12}FN_3O_3$	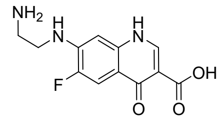
J	5.98	222.04	$C_{10}H_7FN_2O_3$	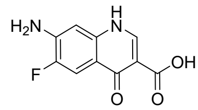
K	4.42	208.06	$C_{10}H_9FN_2O_2$	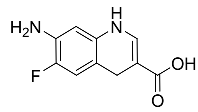

Figures

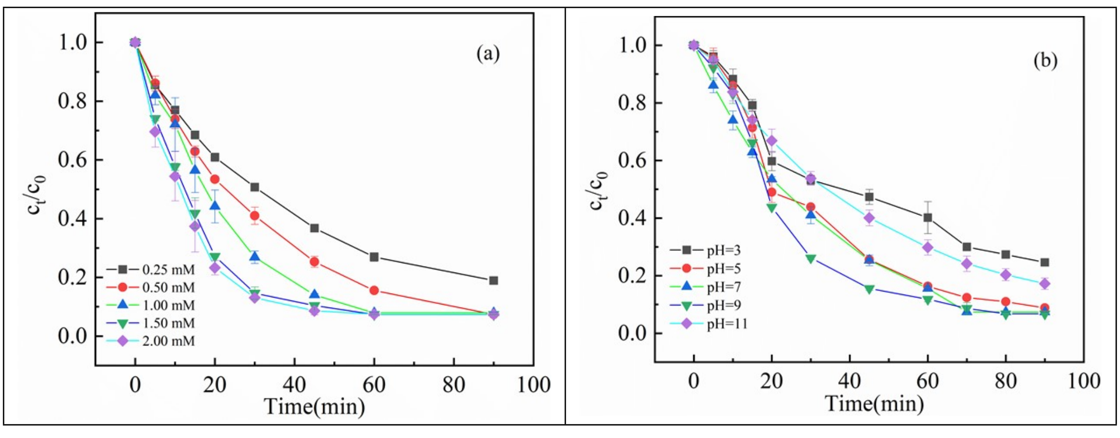

Fig. S2 Effect of (a) initial NH_2Cl concentration, (b) initial pH, of different concentrations on the degradation of CIP by UV/NH_2Cl. Conditions: [CIP] = 19.58 μM = 5mg/L, [NH_2Cl] = 0.25 ~ 2 mM, pH = 5.0 ~ 10.0, [NOM]=0 ~ 4 mg/L, [HCO_3^-]=0 ~ 4 mM, [CO_3^{2-}]=0 ~ 4 mM, [Cl^-]=0 ~ 4 mM, [NO_3^-]=0 ~ 4 mM, [TBA]=0 ~ 50 mM, Is = 65 μW/cm^2.

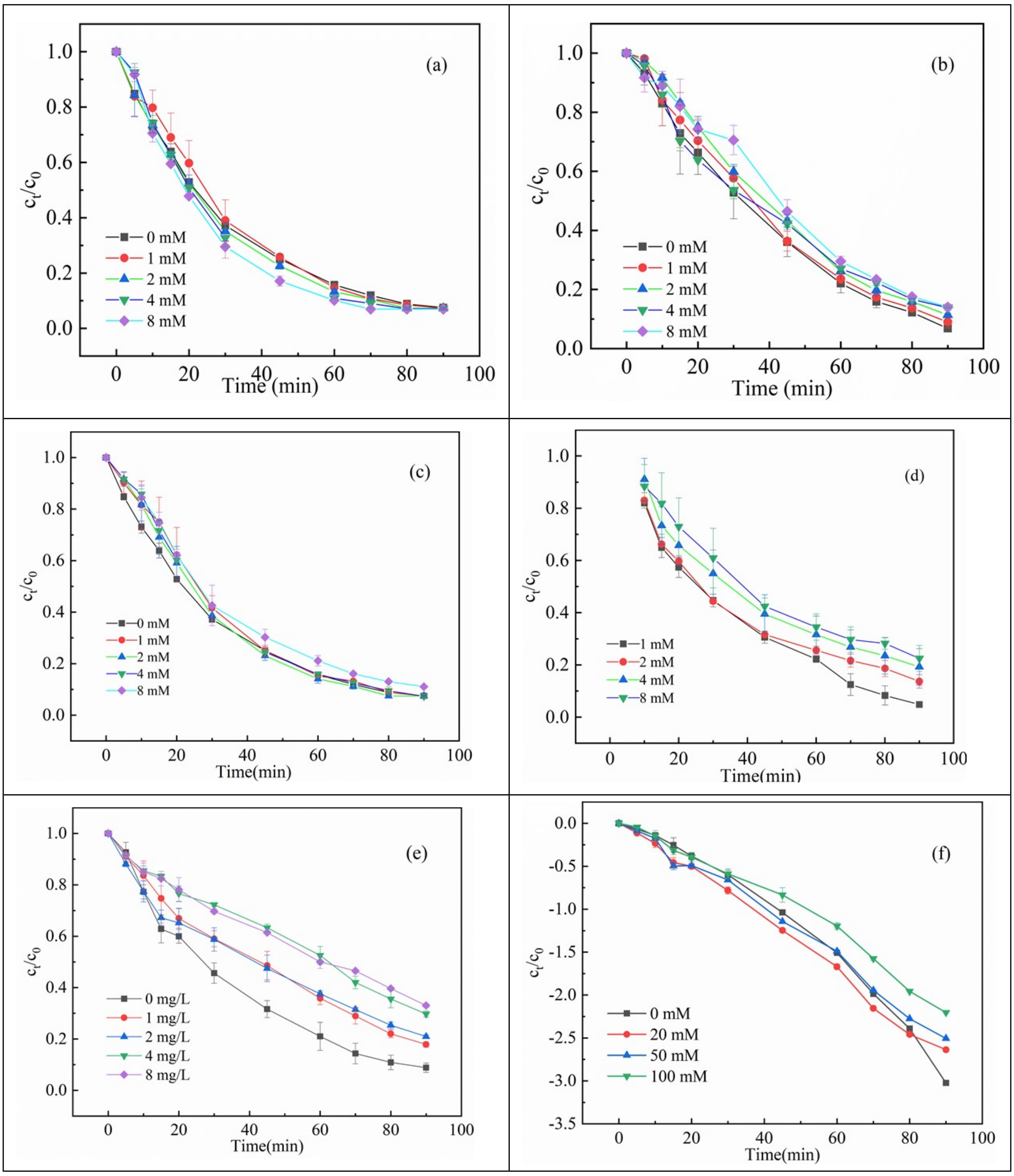

Fig. S3 Effect of (a) Cl^-, (b) NO_3^-, (c) HCO_3^-, (d) CO_3^{2-}, (e) NOM, (f) TBA of different concentrations on the degradation of CIP by UV/NH_2Cl. Conditions: [CIP] = 19.58 μM = 5mg/L, [NH_2Cl] = 0.25 ~ 2 mM, pH = 5.0 ~ 10.0, [NOM]=0 ~ 4 mg/L, [HCO_3^-]=0 ~ 4 mM, [CO_3^{2-}]=0 ~ 4 mM, [Cl^-]=0 ~ 4 mM, [NO_3^-]=0 ~ 4 mM, [TBA]=0 ~ 50 mM, Is = 65 μW/cm^2.

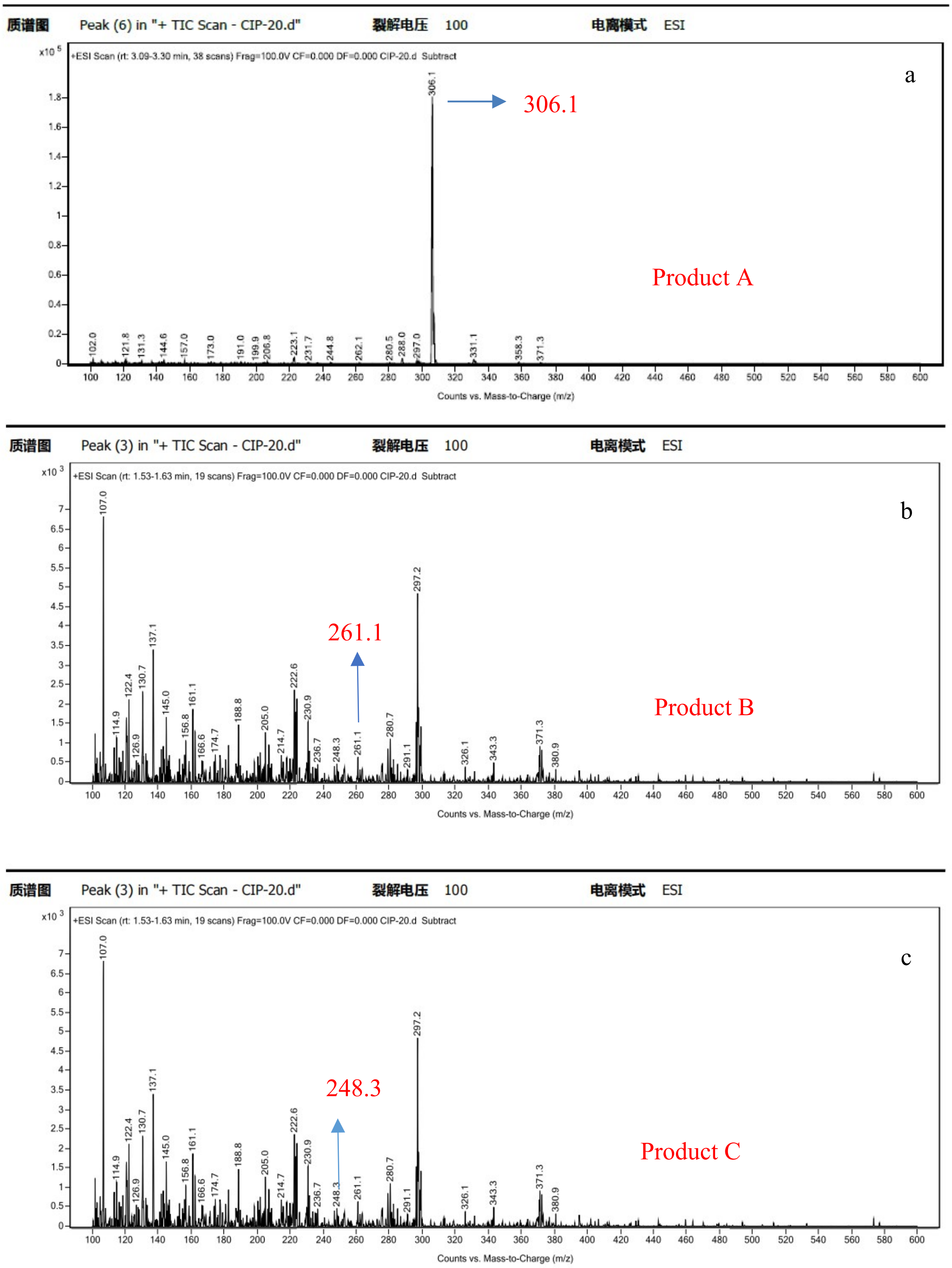
质谱图 Peak (6) in "+ TIC Scan - CIP-20.d" 裂解电压 100 电离模式 ESI
+ESI Scan (rt: 3.09-3.30 min, 38 scans) Frag=100.0V CF=0.000 DF=0.000 CIP-20.d Subtract
a
306.1
Product A
Counts vs. Mass-to-Charge (m/z)
质谱图 Peak (3) in "+ TIC Scan - CIP-20.d" 裂解电压 100 电离模式 ESI
+ESI Scan (rt: 1.53-1.63 min, 19 scans) Frag=100.0V CF=0.000 DF=0.000 CIP-20.d Subtract
b
261.1
Product B
Counts vs. Mass-to-Charge (m/z)
质谱图 Peak (3) in "+ TIC Scan - CIP-20.d" 裂解电压 100 电离模式 ESI
+ESI Scan (rt: 1.53-1.63 min, 19 scans) Frag=100.0V CF=0.000 DF=0.000 CIP-20.d Subtract
c
248.3
Product C
Counts vs. Mass-to-Charge (m/z)

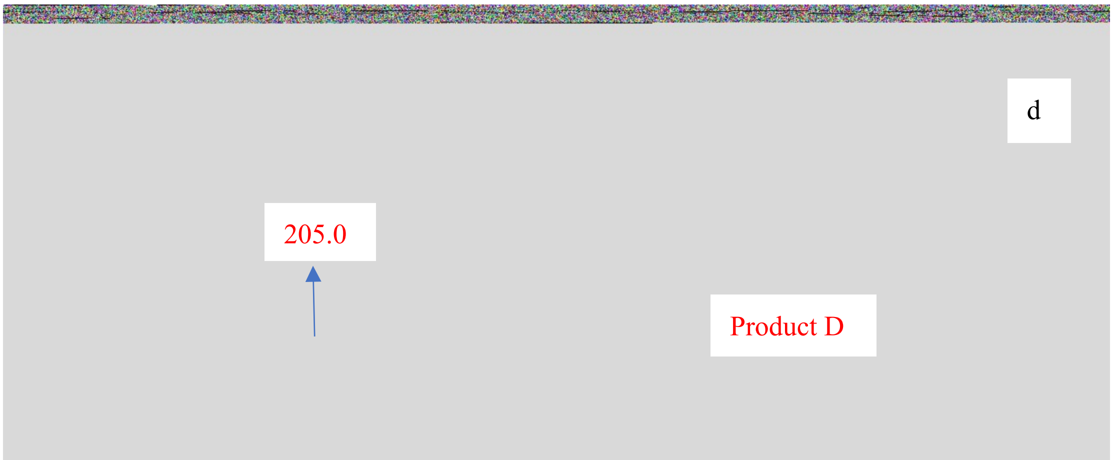
d
205.0
Product D

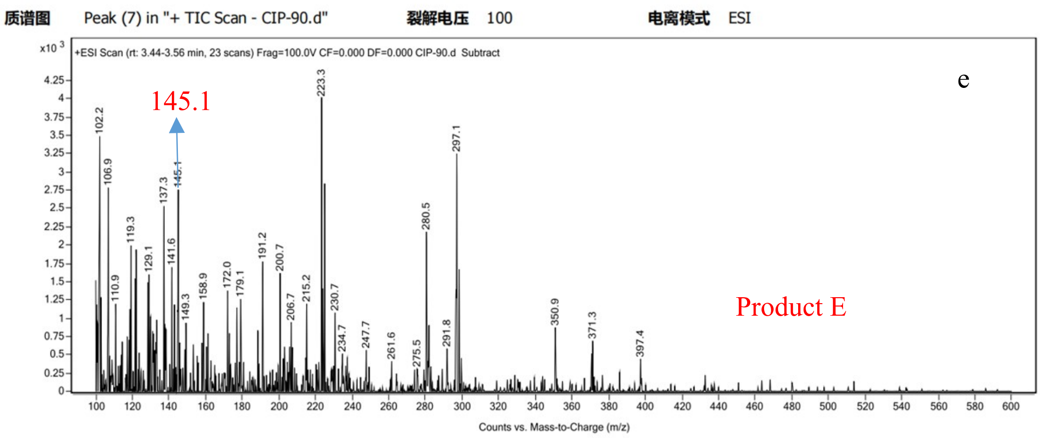
质谱图 Peak (7) in "+ TIC Scan - CIP-90.d" 裂解电压 100 电离模式 ESI
+ESI Scan (rt: 3.44-3.56 min, 23 scans) Frag=100.0V CF=0.000 DF=0.000 CIP-90.d Subtract
e
145.1
Product E
102.2
106.9
110.9
119.3
129.1
137.3
141.6
145.1
149.3
158.9
172.0
179.1
191.2
200.7
206.7
215.2
223.3
230.7
234.7
247.7
261.6
275.5
280.5
291.8
297.1
350.9
371.3
397.4
Counts vs. Mass-to-Charge (m/z)

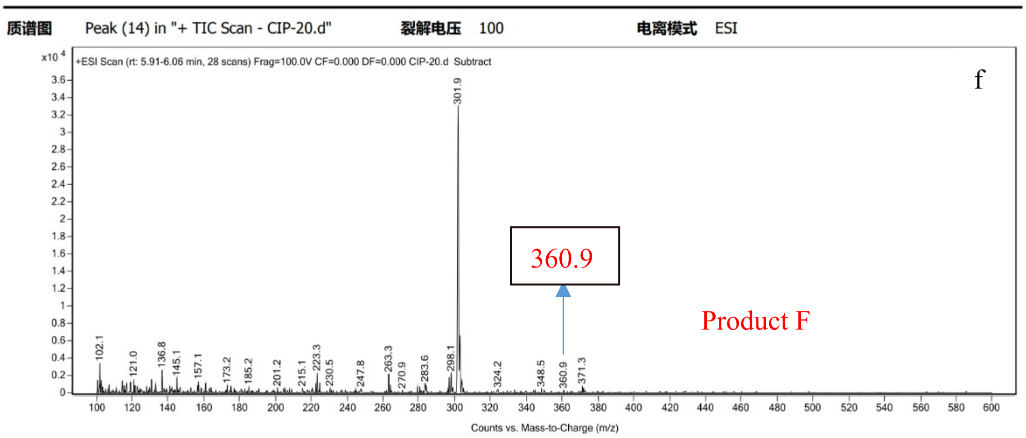
质谱图 Peak (14) in "+ TIC Scan - CIP-20.d" 裂解电压 100 电离模式 ESI
+ESI Scan (rt: 5.91-6.06 min, 28 scans) Frag=100.0V CF=0.000 DF=0.000 CIP-20.d Subtract
f
301.9
360.9
Product F
102.1
121.0
136.8
145.1
157.1
173.2
185.2
201.2
215.1
223.3
230.5
247.8
263.3
270.9
283.6
298.1
324.2
348.5
360.9
371.3
Counts vs. Mass-to-Charge (m/z)

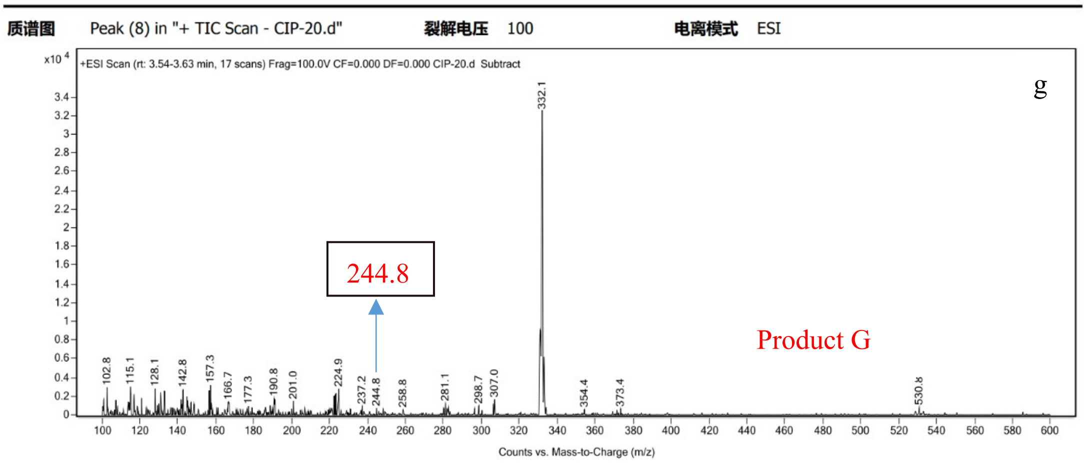
质谱图 Peak (8) in "+ TIC Scan - CIP-20.d" 裂解电压 100 电离模式 ESI
x10 4
+ESI Scan (rt: 3.54-3.63 min, 17 scans) Frag=100.0V CF=0.000 DF=0.000 CIP-20.d Subtract
g
332.1
244.8
Product G
102.8
115.1
128.1
142.8
157.3
166.7
177.3
190.8
201.0
224.9
237.2
244.8
258.8
281.1
298.7
307.0
354.4
373.4
530.8
Counts vs. Mass-to-Charge (m/z)

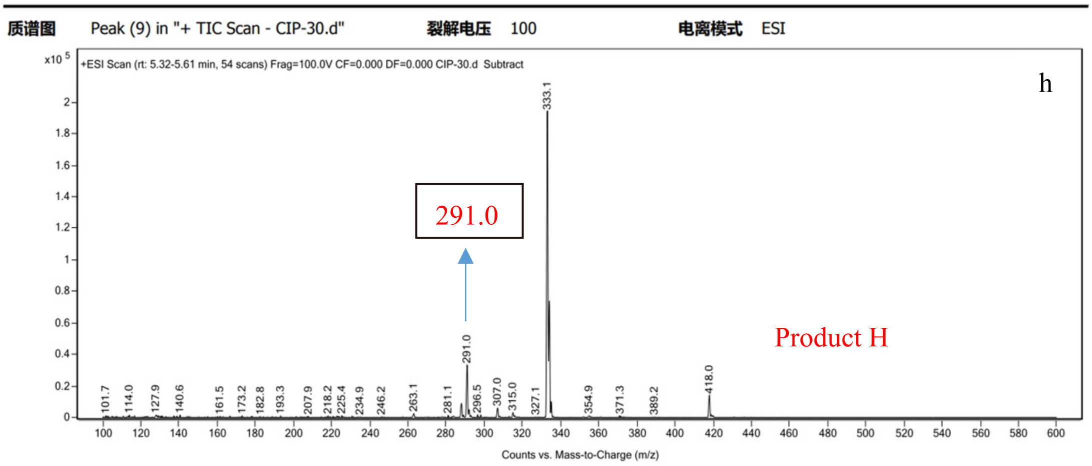
质谱图 Peak (9) in "+ TIC Scan - CIP-30.d" 裂解电压 100 电离模式 ESI
x10 5
+ESI Scan (rt: 5.32-5.61 min, 54 scans) Frag=100.0V CF=0.000 DF=0.000 CIP-30.d Subtract
h
333.1
291.0
Product H
101.7
114.0
127.9
140.6
161.5
173.2
182.8
193.3
207.9
218.2
225.4
234.9
246.2
263.1
281.1
291.0
296.5
307.0
315.0
327.1
354.9
371.3
389.2
418.0
Counts vs. Mass-to-Charge (m/z)

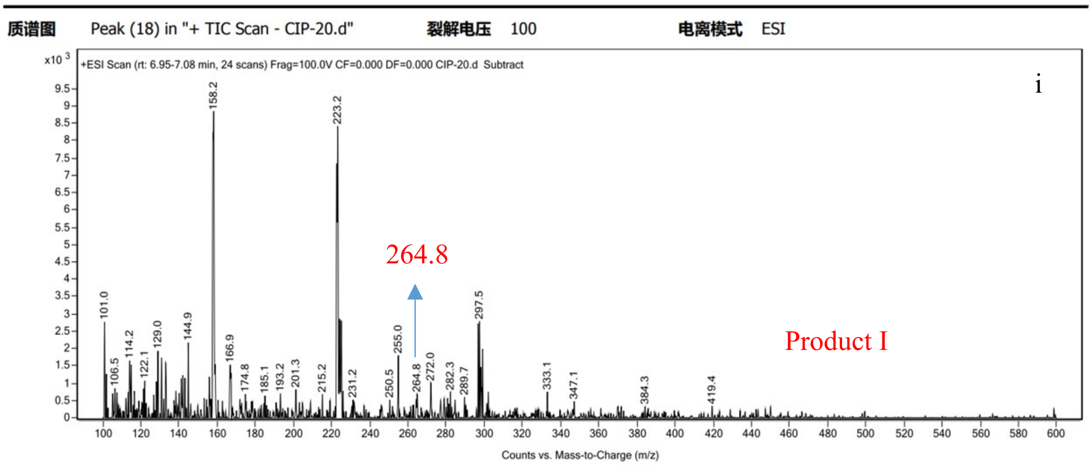
质谱图 Peak (18) in "+ TIC Scan - CIP-20.d" 裂解电压 100 电离模式 ESI
x10 3
+ESI Scan (rt: 6.95-7.08 min, 24 scans) Frag=100.0V CF=0.000 DF=0.000 CIP-20.d Subtract
i
158.2
223.2
264.8
Product I
101.0
106.5
114.2
122.1
129.0
144.9
166.9
174.8
185.1
193.2
201.3
215.2
231.2
250.5
255.0
264.8
272.0
282.3
289.7
297.5
333.1
347.1
384.3
419.4
Counts vs. Mass-to-Charge (m/z)

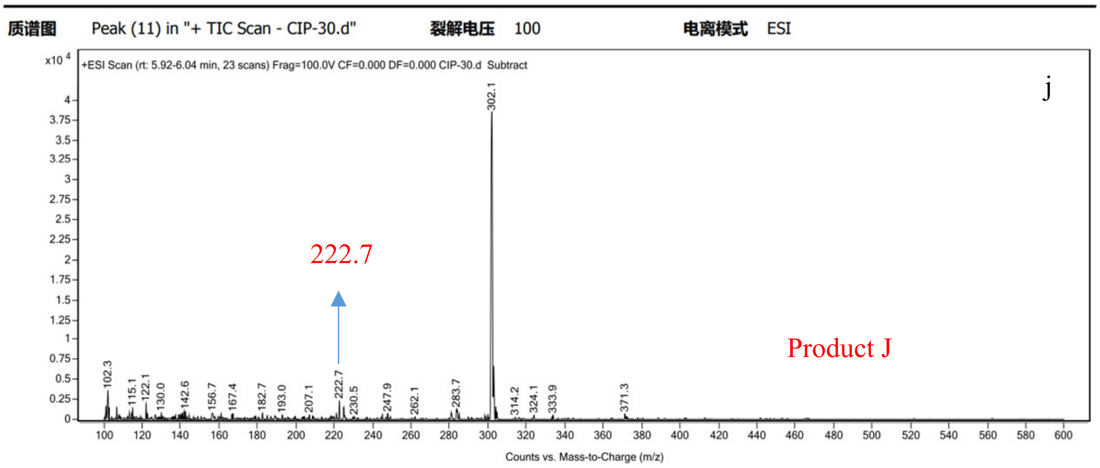
质谱图 Peak (11) in "+ TIC Scan - CIP-30.d" 裂解电压 100 电离模式 ESI
x10 4
+ESI Scan (rt: 5.92-6.04 min, 23 scans) Frag=100.0V CF=0.000 DF=0.000 CIP-30.d Subtract
j
222.7
Product J
102.3
115.1
122.1
130.0
142.6
156.7
167.4
182.7
193.0
207.1
222.7
230.5
247.9
262.1
283.7
302.1
314.2
324.1
333.9
371.3
Counts vs. Mass-to-Charge (m/z)

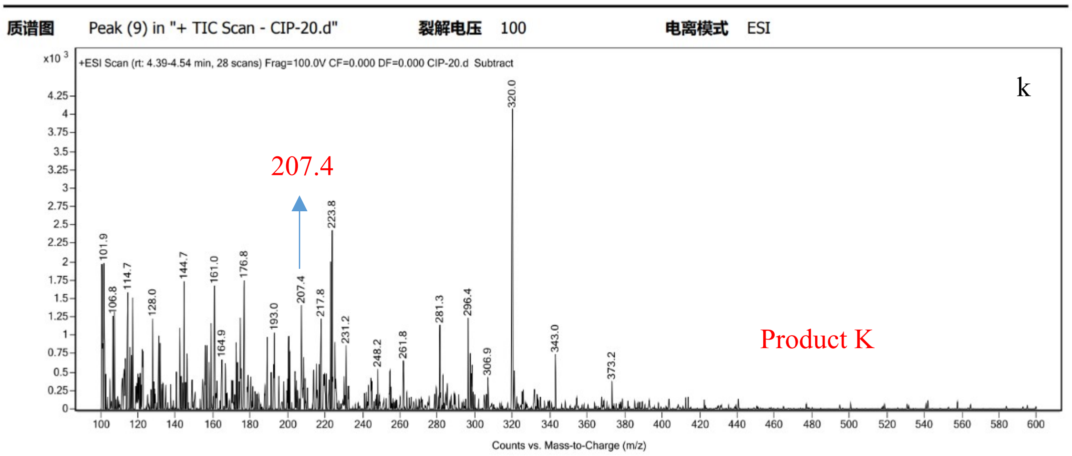
质谱图 Peak (9) in "+ TIC Scan - CIP-20.d" 裂解电压 100 电离模式 ESI
x10 3
+ESI Scan (rt: 4.39-4.54 min, 28 scans) Frag=100.0V CF=0.000 DF=0.000 CIP-20.d Subtract
k
207.4
Product K
101.9
106.8
114.7
128.0
144.7
161.0
164.9
176.8
193.0
207.4
217.8
223.8
231.2
248.2
261.8
281.3
296.4
306.9
320.0
343.0
373.2
Counts vs. Mass-to-Charge (m/z)

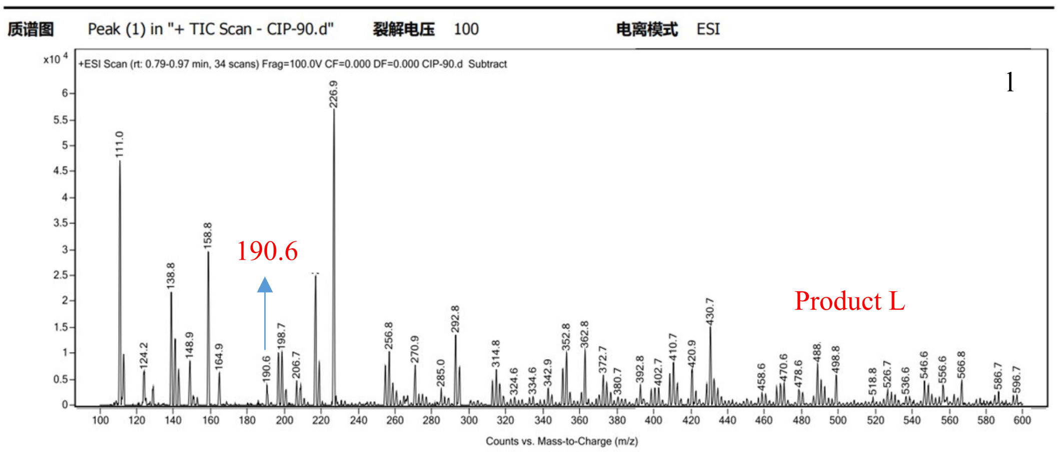
质谱图 Peak (1) in "+ TIC Scan - CIP-90.d" 裂解电压 100 电离模式 ESI
x10 4
+ESI Scan (rt: 0.79-0.97 min, 34 scans) Frag=100.0V CF=0.000 DF=0.000 CIP-90.d Subtract
l
190.6
Product L
111.0
124.2
138.8
148.9
158.8
164.9
190.6
198.7
206.7
226.9
256.8
270.9
285.0
292.8
314.8
324.6
334.6
342.9
352.8
362.8
372.7
380.7
392.8
402.7
410.7
420.9
430.7
458.6
470.6
478.6
488
498.8
518.8
526.7
536.6
546.6
556.6
566.8
586.7
596.7
Counts vs. Mass-to-Charge (m/z)

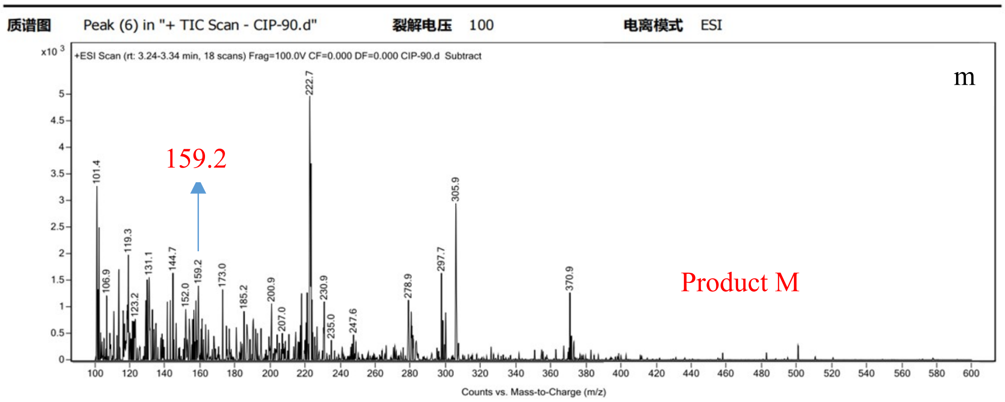

Fig. S3. The mass spectrograms of intermediate products of A to M (a-m).